The HCl–HCl interaction: From quantum mechanical calculations to properties of the liquid

Chr. Votava, R. Ahlrichs, and A. Geiger

Citation: The Journal of Chemical Physics **78**, 6841 (1983); doi: 10.1063/1.444630
View online: http://dx.doi.org/10.1063/1.444630
View Table of Contents: http://aip.scitation.org/toc/jcp/78/11
Published by the American Institute of Physics

The HCl–HCl interaction: From quantum mechanical calculations to properties of the liquid

Chr. Votava, R. Ahlrichs, and A. Geiger[a)]

Institut für Physikalische Chemie und Elektrochemie Universität Karlsruhe, D 7500 Karlsruhe, Federal Republic of Germany

(Received 14 December 1982; accepted 17 February 1983)

Analytical HCl–HCl pair potentials are derived from large quantum mechanical calculations at CEPA-(SD) level. The computed well depth for the dimer is 1.9 kcal/mol. Those pair potentials are used in molecular dynamics simulation studies at $T = 297$ K and $\rho = 0.8354$ g/cm^3. The results for the static (e.g., pair distribution functions) and dynamic properties are compared with experimental and other molecular dynamics results. Comparison of the results from different simulation runs allows a check on their sensitivity with respect to the pair potential employed. It turns out that the potential yielding the best fit to the computed interaction energies gives a good representation of properties of liquid HCl. However, a readjustment of this potential—in order to account for well-known deficiencies of the quantum mechanical calculations—results in a slight improvement especially in the mean potential energy and the pressure. Finally, we used the computed pair potential to determine the structure and association energy of $(HCl)_n$ clusters with cyclic and chain structure.

I. INTRODUCTION

In this paper we report investigations of the structure and properties of liquid HCl by means of pair-potentials obtained from large scale electronic structure calculations. The advantage of this procedure—as compared to empirical approaches—is that quantum-mechanical computations constitute a well defined method, the accuracy of which can be considered as being well under control as a result of an accumulated body of experience. In this sense the development of pair potential models based on the computations performed and the dependence of molecular dynamics results on slight differences in the potentials used are the two main topics of this study.

During the last years several computer simulation studies of liquid hydrogen chloride have been published.[1–5] These investigations were based on pair potentials derived from small basis set SCF computations (which neglect dispersion forces) or by fitting a reasonable Ansatz to experimental data. In a previous paper[6] we have reported CI-level computations of the intermolecular HCl$\cdots$HCl interaction energy for a total of 100 dimer configurations and suggested an analytical potential model, which provided a good representation of the calculated values. However, a closer inspection showed that this first potential-model leads to a minimum energy configuration, which could not be confirmed by additional computations.

In Sec. II we briefly summarize the main features of the electronic structure calculations performed and discuss the results of some supplementary computations which were deviced to probe mainly, the vicinity of the absolute minimum of the dimer energy surface. Using this extended set of interaction energies, two new pair-potential models have been derived which are described in Sec. III. Subsequently, several molecular dynamics simulation runs were carried out to test the capability of these three pair-potential models in reproducing the properties of liquid HCl. The observed discrepancies between theory and experiment (recent neutron diffraction results of liquid HCl by Soper and Egelstaff[7] are available) can be discussed in terms of the approximations inherent to the calculations, such as the neglect of many body effects and the rigid molecule approximation (Sec. IV). In Sec. V we compare the relative stability of various ring and chain clusters calculated on the basis of the "best" pair potential in order to get a better understanding of some IR studies of HCl trapped in a solid matrix.[8]

II. THE COMPUTED HCl PAIR POTENTIAL

In this section we first give a brief survey of the methods and results of our computations of the HCl–HCl interaction, which have been described in more detail in a previous paper,[6] followed by a discussion of the structure and binding energy of the absolute minimum of the hypersurface which we determined by some additional calculations.

The electronic structure calculations were performed at the CI level by means of the CEPA-1-SD method (see, e.g., Ref. 9). The inner shell AO's of the chlorine were simulated by a pseudopotential.[10] The GTO basis for the hydrogen atom was of $(5s/1p)/[3s/1p]$ type with $\eta = 0.3$, for the chlorine atom we used an uncontracted $(4s/4p/2d)$ basis with $\eta_1 = 1.4$ and $\eta_2 = 0.35$.[11]

The HCl molecules were further assumed to be rigid with the intramolecular distance kept at the experimental equlibrium distance of 2.41 a.u.

A detailed study[6] of the nature of the HCl–HCl interaction (explicit tables can be furnished on request) revealed that the angular dependence of the long and medium range part of the hypersurface could be rationalized in terms of the electrostatic interaction which is dominated by the surprisingly large quadrupole mo-

[a)] Present address: Institut für Physikalische Chemie, RWTH Aachen, D 5100 Aachen, Federal Republic of Germany.

 0021-9606/83/116841-08$02.10

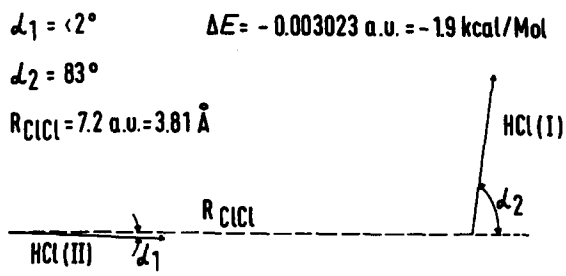

FIG. 1. The computed absolute minimum configuration of the HCl dimer. (The arrow head refers to the H atom.)

ment of the HCl molecule: $\theta_{zz} = 3.75$ D Å. The dipole moment cannot be interpreted as resulting from a shift of electronic charges ($\simeq 0.18$ electrons) from H to Cl because this would yield a quadrupole moment of $\theta_{zz} = 1.4$ D Å only with respect to the chlorine center. θ_{zz} is in fact enhanced by nonisotopic charge distributions around the chlorines since the π electrons are much more diffuse than the σ electrons (as is obvious from the corresponding orbital energies $\epsilon_\sigma = -0.630\,887$ a.u., $\epsilon_\pi = -0.480\,183$ a.u.). This anisotropy of the electron distribution is also reflected in the short range Pauli repulsion, which starts at larger distances for the parallel configuration than it does for the colinear configuration with Cl–Cl approach (see Fig. 1 in Ref. 6). Due to the small anisotropy of the HCl polarizability ($\alpha_\parallel = 2.81$ Å^3, $\alpha_\perp = 2.50$ Å^3)[12] the dispersion energy is nearly isotropic. It has a considerable influence on the position (shift towards shorter intermolecular distances) and the well depth of the minima of the various configurations (which get more pronounced) but not on the angular structure.

The calculations performed in addition to those discussed previously, predict the minimum to be at a nearly orthogonal configuration with a binding energy of -1.9 kcal/mol (Fig. 1). The computed binding energy is in good agreement with the experimental value of -2.14 ± 0.2 kcal/mol, which Rank *et al.*[13] have obtained from ir absorption studies of pure HCl gas in the null gap region.

The discrepancy could be rationalized as being due to mainly two effects:

(i) It is well known that the correlation energy (i.e., the dispersion energy) converges very slowly with the number of polarization functions and is certainly somewhat underrepresented in the given basis set.

(ii) Our calculations are based on rigid HCl molecules. Relaxation of intramolecular geometries—caused mainly by a slight charge transfer from the highest occupied π orbitals of HCl(I) to the lowest unoccupied σ orbitals of HCl(II) (see Fig. 1), which will increase the intramolecular distance of basically HCl(II)—will lead to a deeper well depth.

The nearly orthogonal structure of the dimer is essentially due to the quadrupole–quadrupole interaction. Therefore the structure is well reproduced even by semiempirical[14] and minimal basis set SCF computations,[15] which give a fair representation of electrostatic moments.

III. ANALYTICAL INTERACTION POTENTIALS

In this section we report the consideration leading to the potential models 2 and 3. These potentials have been developed starting from potential 1, which has been published previously.[6]

The electrostatic interaction was represented by the same point charge model for all the potentials considered here. Because of the predominant importance of the quadrupole moment for the HCl molecule at least 3 centers are needed, two located on the H and Cl atoms and the third one (Dummy center) positioned outside the molecule on the side of the Cl atom (see Fig. 2) in order to get a good representation of the computed static potential of an isolated HCl, as discussed in Ref. 6. The total interaction energy V was always written as

$$V = V_1 + V_2 , \tag{1}$$

where V_1 denotes the Coulomb interaction between the point charges. In potential-model 1, V_2 was represented by an atom–atom-type potential, with a Buckingham potential for each atom–atom interaction and an additional attractive term (an exponential function) between the third centers which accounts for the anisotropy of the "Cl electron distribution."

However, this potential model results in an absolute minimum with C_{2h} symmetry, which is too attractive by 600 μhartree as compared with the results of the quantum mechanical computations. Closer inspection revealed that this problem is due to the isotropic Ansatz for the H–H interaction.

A substantial improvement was only achieved, when we added an angle dependent term to the H–H interaction which leads to potential-model 2 (see Table I). This model reproduces the configuration of the calculated absolute minimum with a deviation of less than 60 μhartree in the binding energies.

The virial coefficients, computed with model 2 (see Fig. 3) are shifted towards positive values as compared to the experimental ones.[16] As mentioned in Sec. II our calculations underestimate the dispersion energy. We consequently increased the well depth by augmenting the attractive part of the Cl–Cl interaction in order to get a good representation of the low temperature part of the virial-coefficient curve, which leads to potential-model 3. The remaining deviations in the high temperature part of this curve may be attributed to the fact that we consider only interactions of rigid HCl molecules, i.e., we neglect effects of intramolecular relaxation and vibrational averaging and excitations. Potential 3 leads to a minimum geometry very similar to that of potential

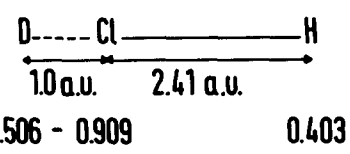

FIG. 2. The electrostatic point-charge model (Q_i denote the charge on the different sites).

TABLE I. The parameters of the three pairpotential models developed and the corresponding minimum energy structure of the dimer.

$V = V_1 + V_2$ V_1 Coulomb interaction between point charges	Minimum-energy configuration for the different potential models (for the definition of the angles see Fig. 1)
potential 1	$\alpha_1 = 40.1°$
$V_2 = 0.132199 \exp[-1.9r(HH')]$ $+113.136242 \exp[-1.6r(ClCl')] - 7219.288073/r(ClCl') + 9$ $+15.168861 \exp[-1.9r(HCl')] - 7.882769/r(HCl') + 5$ $+15.168861 \exp[-1.9r(H'Cl)] - 7.882769/r(H'Cl) + 5$ $-1.088930 \exp[-1.3r(DD')]$	$\alpha_2 = 137.3°$ $R(Cl-Cl) = 6.733$ a.u. $\Delta E = -0.003709$ a.u.
potential 2	
$V_2 = 15.349556 \exp[-1.83r(HH')]$ $-0.871467\{[1+\cos\theta(A)][1+\cos\theta(B)]\} \exp[-1.79r(HH')]$ $+99.821964 \exp[-1.55r(ClCl')] - 123.295206/r(ClCl') + 6$ $+32.555317 \exp[-2.15r(HCl')] - 28.839270/r(HCl') + 6$ $+32.555317 \exp[-2.15r(H'Cl)] - 28.839270/r(H'Cl) + 6$ $-1.810831 \exp[-1.45r(DD')]$	$\alpha_1 = 8.11°$ $\alpha_2 = 87.03°$ $R(Cl-Cl) = 7.10$ a.u. $\Delta E = -0.003084$ a.u.
$\theta(A)$, respectively, $\theta(B)$ is the angle between the Cl–Cl axis and the intramolecular HCl axis, e.g.,: $\theta(A) = -\alpha_1$ and $\theta(B) = (180° - \alpha_2)$.	
potential 3 Just as potential 2 with the only difference that the attractive part of the Cl–Cl interaction is increased, e.g.: $99.821964 \exp[-1.55r(ClCl')] - 160.283768/r(ClCl) + 6$	$\alpha_1 = 8.72°$ $\alpha_2 = 87.49°$ $R(Cl-Cl) = 7.035$ a.u. $\Delta E = -0.003381$ a.u.

2 (see Table I), but the binding energy of potential 3 is now very close to the experimental value. It thus appears that the corrections applied on potential 2 to get potential 3—a slight readjustment of just one parameter to remedy known deficiencies of the computational procedures—leads to a consistent improvement.

In Fig. 3 we also include the virial coefficients as obtained with two other potential models called C and C^* developed by McDonald *et al.*[1] and Klein *et al.*[2] Potential C, although fitted to the second virial coefficient, leads to deviations of 20–50 cm^3/mol along the whole curve. Potential C^*, derived from potential C and slightly readjusted in order to reproduce the experimental structure of liquid HCl obtained by Soper and Egelstaff,[7] leads to similar deviations. These problems indicate the difficulty to conceive reliable potential models even for a simple case as the HCl dimer, and large basis set calculations can be of great help in this respect.

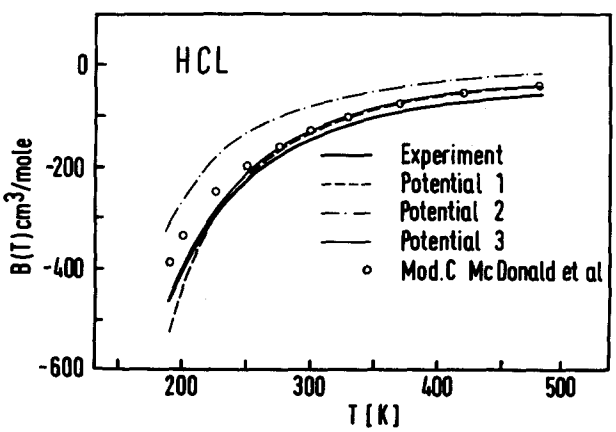

FIG. 3. Second virial coefficient of gaseous HCl. The solid line shows the experimental data (Ref. 15), the broken lines refer to potential-models 1, 2, 3 and the circles to potential-model C (Ref. 1).

IV. RESULTS OF MOLECULAR DYNAMICS SIMULATION STUDIES

A series of MD calculations was performed in order to study in more detail the quality of the potentials described above.

Soper and Egelstaff[7] have recently determined the atom–atom pair distribution functions of liquid HCl at a density of $\rho = 0.8354$ g/cm^3 and a temperature of $T = 297$ K by means of neutron diffraction studies of samples with different isotopic compositions. Molecular dynamics calculations were performed for systems of 216 molecules contained in a cubic box with periodic boundary conditions at the experimental density and near the experimental temperature using potentials 1 to 3. The potentials were truncated at half the box length. The spherical cutoff can be justified by the predominancy of the quadrupole moment over the dipole moment for

the HCl molecule. In the computations we further used the method of constraints[17] in connection with the Verlet algorithm.[18] Starting with an equilibrated sample each simulation run covered time periods of approximately 4.2 ps, corresponding to 2100 time steps.

A. Static properties

The atom–atom pair distribution functions obtained with the three potential models developed in this work are compared in Fig. 4(a)–4(c) with the experimental ones and with those published by Klein and McDonald (potential C^*).[2] The potentials 1–3 reproduce perfectly the first peak of $g_{Cl-Cl}(r)$. This indicates, that they yield a satisfactory description of the short range part of the interaction. The second peak of this distribution function is shifted for all three potentials by about 0.5 Å to larger distances as compared to experiment. The double-hump shape of $g_{Cl-H}(r)$ can be interpreted by the configuration of the absolute minimum (Fig. 1): the first shoulder corresponds to the "hydrogen bond" and the second peak to the "free" $H_{II}-Cl_I$ approach. Whereas the second peak is in excellent agreement with the experiment for the potentials 2 and 3 the shoulder is reproduced with less intensity.

The strongest deviation can be seen for $g_{H-H}(r)$ where the experimentally determined distribution function indicates a more ordered structure than the results of our simulations.

We cannot offer a quantitative explanation of the deviations between experimental and the present theoretical results. The theoretical treatment could suffer from deficiencies of the electronic structure calculations (e.g., basis sets, pseudopotential approximation), neglect of bond length relaxation and of many body effects. As to the uncertainties of neutron diffraction data we refer to the literature.[7,19]

The tendency of potential 1 to underestimate the H–H repulsive forces and to favor an antiparallel minimum energy configuration is reflected in the shape of both the Cl–H and the H–H pair-distribution functions. Compared to the potentials 2 and 3 the more intensive first and the less intensive second peak of $g_{Cl-H}(r)$ exhibits an increased number of closer Cl–H contacts whereas the rise of $g_{H-H}(r)$ at shorter distances indicates closer H–H approaches.

Potential C^* of Klein and McDonald,[2] although describing accurately the overall shape of the pair correlation functions, fails in reproducing some important features of the structure, like the intensity of the first peak of $g_{Cl-Cl}(r)$. Moreover, because of the fact that C^* is an adjusted empirical effective pair potential, it is quite difficult to extract the reasons of the deviations from the experimental results.

These discussions show potentials 2 and 3 to be equally well suited to reproduce the structure of liquid HCl. In Table II we list additional properties obtained from our molecular dynamics simulations. The adjustments made to derive potential 3 from potential 2 lead to a marked improvement in the mean potential energy E_{pot} and the pressure p. (Both have been corrected for the

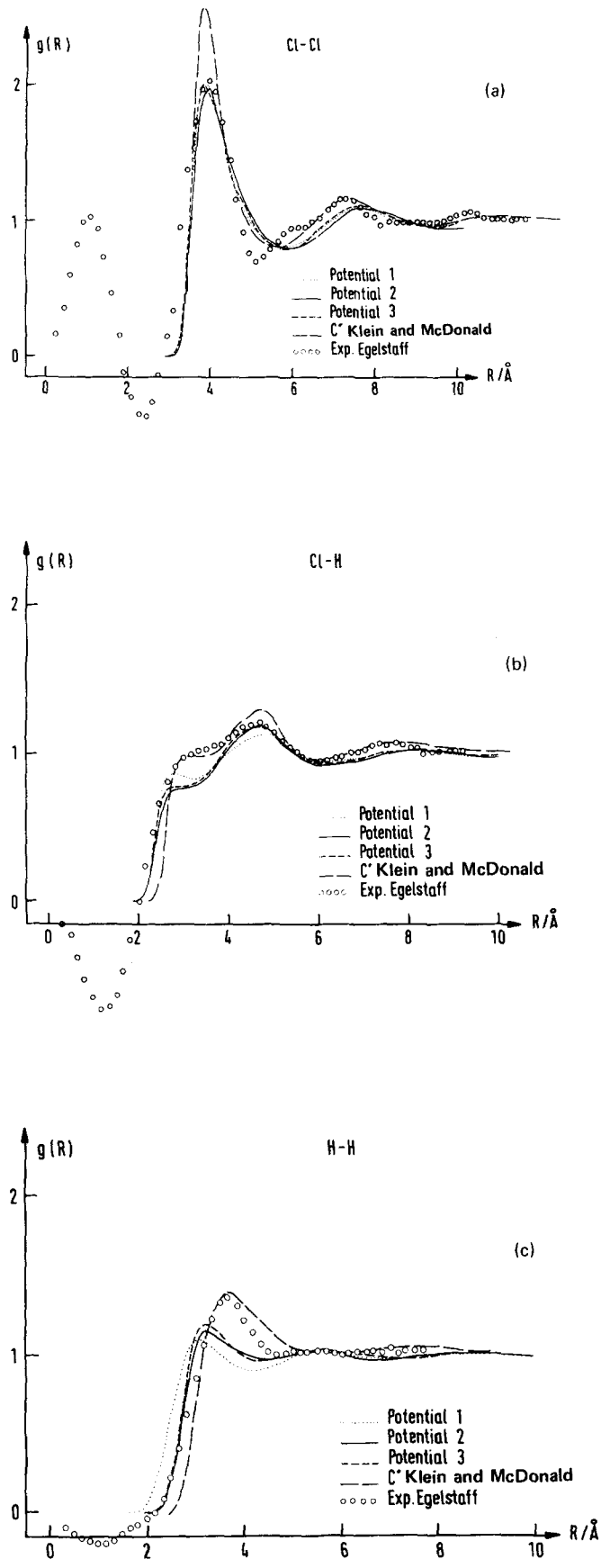

FIG. 4. (a)–(c) Atomic radial distribution functions $g_{Cl-Cl}(R)$, $g_{Cl-H}(R)$ and $g_{H-H}(R)$, for potential models 1, 2, 3 and potential-mdoel C^* (Ref. 2). The circle show the experimental data (Ref. 7).

TABLE II. Molecular dynamics results of liquid HCl for different potential models; static properties.

	T [K]	E [kcal/mol]	p [atm]	c_v [cal/Kg]	G	g,
Potential 1	300	−2.20	690	a	0.50	0.79
Potential 2	301	−1.86	1040	0.21	0.66	1.06
Potential 3	304	−2.33	440	0.23	0.73	1.18
Potential C*	296	−2.28	380			
Expt.	297	−2.48	55	0.20		1.20
		Ref. 5	Ref. 29	Ref. 29		Ref. 23

[a]This value was not computed due to a disk failure.

interaction cutoff, using a procedure proposed by Stillinger and Rahman.[20])

Compared to the experimental value, even potential 3 shows deviations which indicate a lack of cohesivity. This could be attributed to the fact that our potentials neglect additional attractive contributions from many-body interactions and bond length relaxation, as already discussed.

In contrast to E_{pot} and p, the specific heat C_v, calculated via the temperature fluctuations,[21] is found to be rather independent of the dispersion part of the interaction and to be very close to the experimental value.

The last two columns of Table II show the orientational correlation factor $G=\langle M^2\rangle/N$ for the finite $N=216$ particle system (if $\hat{\mu}_i$ denotes the unit vector along the dipole moment direction for molecule i, then $M=\sum_i \hat{\mu}_i$) and the Kirkwood g factor g. The Kirkwood g factor is derived from G in using a method described by Rahman and Stillinger,[22] which requires the knowledge of the dielectric constant ϵ_0 taken from Ref. 23.

Potential 1 leads to a g factor smaller than 1, which confirms in fact the tendency of this potential to favor an antiparallel orientation of nearest neighbor molecules, whereas potentials 2 and 3 apparently reproduce the dielectric properties of the liquid. The close agreement between the g factor for potential 3 and the experimental value is certainly fortuitous to some extent.

B. Dynamic properties

In a next step we studied the capability of the three potentials to reproduce the microdynamic behavior of the liquid. For this purpose we determined the reorientational correlation functions

$$\Gamma_i(t)=\langle P_i(\hat{\mu}_j(t_0)\cdot\hat{\mu}_j(t_0+t))\rangle\ ,\quad \text{with } i=1,2\ , \tag{2}$$

where $P_i(\cos\theta)$ is the Legendre polynomial of order i and $\hat{\mu}_j$ the dipole direction unit vector of molecule j. The corresponding correlation times τ_i have been determined by numerical integration of $\Gamma_i(t)$:

$$\tau_i=\lim_{t'\to\infty}\int_0^{t'}\Gamma_i(t)\,dt\ . \tag{3}$$

The values given in Table III are of course subject to errors of approximately 20%, since we only observed a time period of 4.2 ps with finite time intervals of 2×10^{-15} s. The self-diffusion coefficient D was determined from the mean-square displacements. The experimental values for τ_2 and D are taken from NMR experiments of Krynicki *et al.*[24,25]

The microscopic mobility decreases from potential 1 to potential 3 (see the values of τ_1 and D). On first glance this appears to be at variance with the well depth of the pair potentials (see Table I). However, there is no direct systematic relationship between the well depth of the potentials on one side and the values of τ_1 and D on the other since the latter are determined by the N-particle potential surface.

τ_2 seems to be much less sensitive to the differences in the potentials. This might be rationalized by the fact that τ_2 probes mainly the reorientations about smaller angles, which is nearly free as will be seen below and therefore only slightly model dependent.

In Fig. 5 we compare different $\Gamma_2(t)$ curves. One is taken from our simulations study with potential 3 and one results from a simulation of Powles *et al.*[5] for orthobaric HCl at 284 K using a double Lennard-Jones potential adjusted to thermodynamic data (this potential fails to reproduce some important structural features like the first shoulder in $g_{Cl-H}(r)$, which is to be attributed to the "hydrogen-bond"[26]). The third $\Gamma_2(t)$ curve of Fig. 5 was obtained from Raman scattering spectra for orthobaric HCl at 295 K.[27] It leads to a correlation time τ_2 which is clearly above the NMR value.

The results of the molecular dynamics simulations show a fast initial decay, which indicates almost free rotation over appreciable angles, followed by a slow and

TABLE III. Molecular dynamics results of liquid HCl for different potential models; dynamic properties.

	T [K]	τ_1 [10^{-13} s]	τ_2 [10^{-13} s]	D [10^{-5} cm^2 s^{-1}]
Potential 1	300	1.2	0.7	18.5
Potential 2	301	1.6	0.6	16.3
Potential 3	304	2.0	0.6	15.5
Expt.	304		0.61 Ref. 25	20–24 Ref. 24

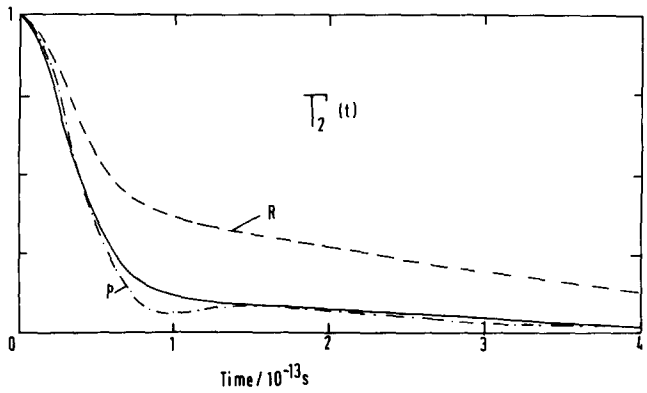

FIG. 5. Reorientational correlation function $\Gamma_2(t)$ for potential 3 (solid line). The line labeled R refers to light scattering results (Ref. 27), the one labeled P to molecular dynamics simulations of Powles *et al.* (Ref. 5).

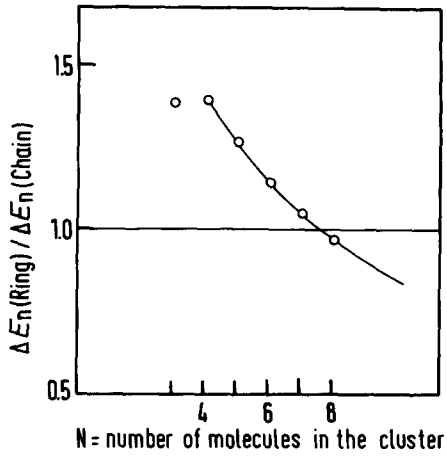

FIG. 7. Relative stability of ring clusters opposite to chain clusters.

nearly exponential decay. The agreement among the molecular dynamics results is not as good as it appears on first glance, since the temperature of the two simulations differ by 19 K. However, despite some uncertainties due to the just mentioned temperature differences, our results support the NMR results and cannot be reconciled with light-scattering results (which indicate a much slower reorientational behavior), as has already been stated by Powles *et al.*[5]

V. STRUCTURE AND GEOMETRY OF HCl OLIGOMERS

On the basis of potential 2—the best fit to the computed points of the dimer surface—we studied the structure and stability of ring and chain clusters containing up to 8 HCl molecules in order to bridge the gap from the gas-phase dimer structure and the liquid structure to the structure of solid HCl. We optimized the cluster energy—computed as the sum of the corresponding pair-potentials—with respect to the geometry, where we only considered the local minima in the neighborhood of a reasonable guess for the ring and chain structure. No other local minima were detected, but a thorough search is prohibitive by virtue of the large dimensions of the corresponding configuration spaces.

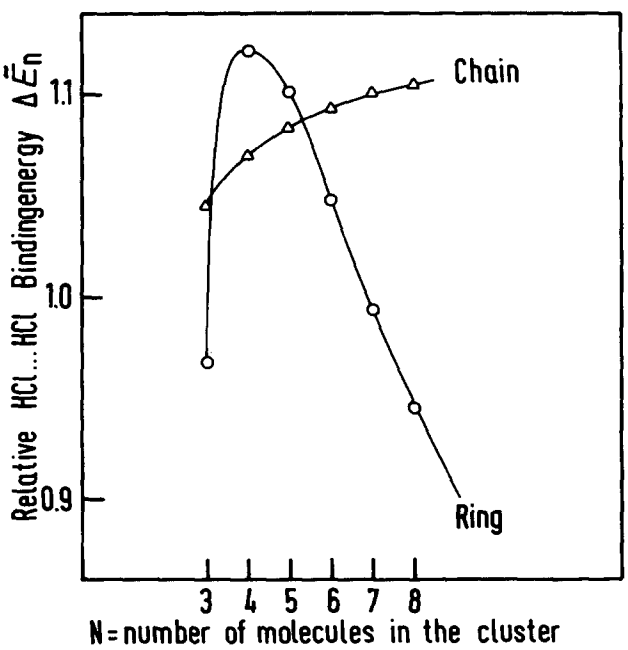

FIG. 6. Relative HCl–HCl binding energy as a function of ring and chain size.

In Fig. 6 we plotted the average HCl–HCl binding energy $\Delta\tilde{E}_n$ in units of the pair-binding energy ΔE_2 (compare Table I) as a function of the ring and chain size. If ΔE_n denotes the corresponding cluster energy (with respect to n separated HCl molecules) than

$$\Delta\tilde{E}_n = \frac{\Delta E_n}{(n-1)\Delta E_2} \quad \text{for rings,} \tag{4a}$$

$$\Delta\tilde{E}_n = \frac{\Delta E_n}{n\Delta E_2} \quad \text{for chains .} \tag{4b}$$

The interaction between the molecules is thus most favorable for an $(HCl)_4$ ring. For larger rings the relative HCl–HCl bond gets weaker because of the unfavorable orientation between adjacent molecules (Angle $> 90°$) and the increased distance to opposite molecules (decrease in long range Coulomb interactions), whereas for a 3 molecule ring the "ringstrain" weakens the bond. For chains the binding energy to each additional molecule is always larger than for the dimer due to the attractive Coulomb type interaction to the non-next neighbors. However, this effect tends to converge towards a threshold.

In Fig. 7 we compare ΔE_n for ring and chain structures. It turns out that rings containing less than 6 molecules are more stable than the corresponding chains. This is due to the additional bond in the rings arising from the ring closure. The preponderant stability of the cyclic trimer and tetramer is also confirmed by IR studies of HCl in solid matrices performed by Maillard *et al.*[8] These authors could not detect any other oligomeric species as just these two cycles with C_{3h} and C_{4h} symmetry, respectively. For the sake of completeness we give the optimized structure parameters and energies for the investigated clusters in Table IV. Ac-

TABLE IV. Optimized structure parameter and energies for the investigated clusters [for the meaning of $R = R_{Cl-Cl}$, α, β and γ see Figs. 8(1) and 8(b)].

Rings	$n=3$	$R=7.07$	$\beta=60°$	$\alpha=+19°$	$\Delta E=-0.008\,963$
	$n=4$	$R=7.04$	$\beta=90°$	$\alpha=+6°$	$\Delta E=-0.013\,834$
	$n=5$	$R=7.04$	$\beta=108°$	$\alpha=-2°$	$\Delta E=-0.016\,986$
	$n=6$	$R=7.04$	$\beta=120°$	$\alpha=-7°$	$\Delta E=-0.019\,392$
	$n=7$	$R=7.04$	$\beta=51.4°$	$\alpha=-11°$	$\Delta E=-0.021\,455$
	$n=8$	$R=7.05$	$\beta=45°$	$\alpha=-14°$	$\Delta E=-0.023\,338$
Chains	$n=3$	$R_1=7.08$	$\beta_2=90.1°$	$\alpha_1=+9.5°$	$\Delta E=-0.006\,450$
		$R_2=7.08$	$\gamma=99.7°$	$\alpha_2=-1.3°$	
	$n=4$	$R_1=7.08$	$\beta_2=89.7°$	$\alpha_1=+8.5°$	$\Delta E=-0.009\,904$
		$R_2=7.23$	$\beta_3=97.3°$	$\alpha_2=+0.0°$	
		$R_3=7.22$	$\gamma=96.3°$	$\alpha_3=+1.4°$	
	$n=5$	$R_1=7.08$	$\beta_2=91.3°$	$\alpha_1=+8.3°$	$\Delta E=-0.013\,372$
		$R_2=7.05$	$\beta_3=99.7°$	$\alpha_2=-1.4°$	
		$R_3=7.06$	$\beta_4=97.5°$	$\alpha_3=+2.7°$	
		$R_4=7.07$	$\gamma=98.8°$	$\alpha_4=-1.9°$	
	$n=6$	$R_1=7.08$	$\beta_2=90.7°$	$\alpha_1=+8.6°$	$\Delta E=-0.016\,854$
		$R_2=7.05$	$\beta_3=96.6°$	$\alpha_2=-1.5°$	
		$R_3=7.05$	$\beta_4=102.6°$	$\alpha_3=+0.2°$	
		$R_4=7.06$	$\beta_5=95.3°$	$\alpha_4=-4.4°$	
		$R_5=7.08$	$\gamma=99.5°$	$\alpha_5=+1.3°$	
	$n=7$	$R_1=7.08$	$\beta_2=93.3°$	$\alpha_1=+7.2°$	$\Delta E=-0.020\,361$
		$R_2=7.05$	$\beta_3=97.7°$	$\alpha_2=-2.0°$	
		$R_3=7.05$	$\beta_4=98.5°$	$\alpha_3=+1.5°$	
		$R_4=7.05$	$\beta_5=99.8°$	$\alpha_4=-1.8°$	
		$R_5=7.05$	$\beta_6=96.9°$	$\alpha_5=+3.2°$	
		$R_6=7.07$	$\gamma=99.1°$	$\alpha_6=-1.7°$	
	$n=8$	$R_1=7.08$	$\beta_2=90.9°$	$\alpha_1=+7.2°$	$\Delta E=-0.023\,864$
		$R_2=7.05$	$\beta_3=92.3°$	$\alpha_2=-1.8°$	
		$R_3=7.05$	$\beta_4=98.1°$	$\alpha_3=+1.7°$	
		$R_4=7.05$	$\beta_5=97.3°$	$\alpha_4=-1.9°$	
		$R_5=7.05$	$\beta_6=100.7°$	$\alpha_5=+1.2°$	
		$R_6=7.05$	$\beta_7=96.5°$	$\alpha_6=-3.5°$	
		$R_7=7.07$	$\gamma=98.7°$	$\alpha_7=+1.5°$	

cording to our investigations (see above) the minimum energy structure of large clusters is a zig-zag chain, which already bears a close resemblance to the structure of solid HCl, also composed of zig-zag chains with $R=6.9694$ a.u., $\theta=93.5°$, and $\alpha=0.0°$.[28]

VI. SUMMARY AND CONCLUSIONS

In this paper extended CEPA calculations for the HCl dimer are reported. The computed association energy is found to be 1.9 kcal/mol.

Analytical expressions were developed to reproduce the interaction between two rigid HCl molecules. Potential 2 was the best fit to all computed points of the hypersurface, while potential 1 gives a relatively poor representation of the minimum.

As it turned out, the dispersion energy contribution is somewhat underrepresented in our calculations, which is certainly not an unexpected fact. In order to get a better representation of the second virial coefficient one term of potential 2 was readjusted, which lead to potential 3.

With the three pair-potentials molecular dynamics simulations of liquid HCl were performed. The potentials 2 and 3 reproduce equally well the main features of the structure of the liquid.

Since potential 3 yields slightly superior results for thermodynamic data it gives the best overall description of the potentials discussed here.

The computed dynamic properties of the liquid are in good agreement with the available experimental values. Furthermore the computed reorientational correlation—function $\Gamma_2(t)$ is much closer to the one obtained by NMR—than by light-scattering experiments. This suggests, as already conjectured by Powles *et al.*,[5] a systematic error in the interpretation of these light-scattering experiments.

The cluster structures computed on the basis of potential 2 indicate the stability of trimer and tetramer for smaller clusters whereas for larger clusters a zig-zag chain, which is very similar to the solid structure, is the most stable aggregate.

To sum up: Theoretical pair potentials such as potential 2—which described the interaction between two isolated HCl molecules and deviate appreciably from empirical potentials—lead to a surprisingly accurate description of properties of liquid HCl. A slight im-

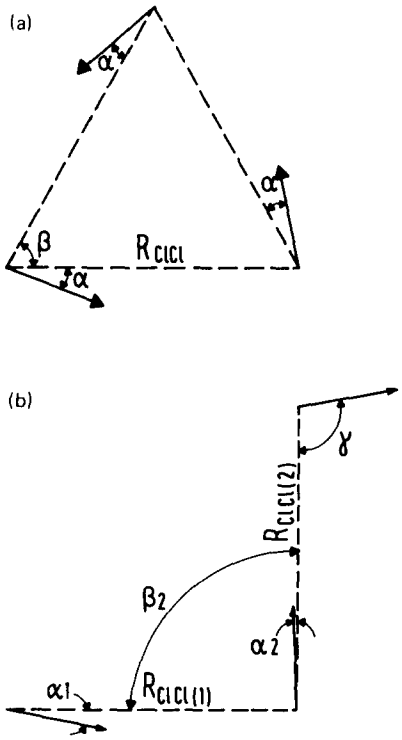

FIG. 8. (a,b) The minimum-energy structure of 3-membered ring and chain clusters.

provement could be obtained by a minor readjustment of the computed potential, which may correct well known deficiencies of CI-type calculations of intermolecular forces. In a next step, one would have to investigate thoroughly the influence of bond length relaxation on the properties of the liquid, before attacking the many body effect problem.

ACKNOWLEDGMENTS

The authors thank P. Scharf and P. Weber for valuable assistance in the study of HCl oligomers, and J. Böhm for help in preparing the manuscript. The computations were performed at the "Rechenzenztrum der Universität Karlsruhe." This work was supported by the "Deutsche Forschungsgemeinschaft" (project He131/23), and in part by the "Fond der Chemischen Industrie."

[1]I. R. McDonald, S. F. O'Shea, D. G. Bounds, and M. L. Klein, J. Chem. Phys. **72**, 5710 (1980).
[2]M. L. Klein and I. R. McDonald, Mol. Phys. **42**, 243 (1981).
[3]J. G. Powles, W. A. B. Evans, E. McGrath, K. E. Gubbins, and S. Murad, Mol. Phys. **38**, 893 (1979).
[4]S. Murad, K. E. Gubbins, and J. G. Powles, Mol. Phys. **40**, 253 (1980).
[5]J. G. Powles, E. McGrath, and K. E. Gubbins, Mol. Phys. **40**, 179 (1980).
[6]Chr. Votava and R. Ahlrichs, in *Intermolecular Forces, Proceedings of the Fourteenth Jerusalem Symposium*, edited by B. Pullmann; (D. Reidel, Dordrecht, 1981).
[7]A. K. Soper and P. A. Egelstaff, Mol. Phys. **42**, 399 (1981).
[8]D. Maillard, A. Shriver, J. P. Perchard, and C. Girardet, J. Chem. Phys. **71**, 517 (1979).
[9](a) C. Zirz and R. Ahlrichs: *Recent Developments in Coupled Pair Theories* in Electron Correlation, proceedings of the Daresbury Study Weekend, 17–18 November 1979, edited by M. F. Guest and S. Wilson. (b) W. Meyer, J. Chem. Phys. **58**, 1017 (1972); (c) W. Kutzelnigg, in *Modern Theoretical Chemistry*, edited by H. F. Schaefer III (Plenum, New York, 1977), Vol. III; (d) R. Ahlrichs, Comput. Phys. Commun. **17**, 31 (1979).
[10]T. C. Chang, P. Habitz, B. Pittel, and W. H. E. Schwarz, Theor. Chim. Acta **34**, 263 (1974).
[11]S. Huzinaga, "Approximate Atomic Functions I/II," Department of Chemistry of the University of Alberta, Canada.
[12]N. J. Bridge and A. D. Buckingham, Proc. R. Soc. London Ser. A **295**, 334 (1966).
[13]D.H. Rank, P. Sitaram, W. A. Flickman, and T. A. Wiggins, J. Chem. Phys. **39**, 2673 (1963).
[14]A. Shriver, D. Maillard, and B. Silvi, Chem. Phys. Lett. **54**, 514 (1978).
[15]P. Kollman, A. Johansson, and S. Rothenberg, Chem. Phys. Lett. **24**, 199 (1974).
[16]B. Schramm and U. Leuchs, Ber. Bunsenges. **83**, 847 (1979).
[17]J. P. Ryckaert, G. Ciccotti, and H. J. C. Berendsen, J. Comput. Phys. **23**, 327 (1977).
[18](a) A. Verlet, Phys. Rev. **159**, 98 (1967); (b) W. F. van Gunsteren and H. J. Berendsen, Mol. Phys. **34**, 1311 (1977).
[19]P. A. Egelstaff, in *Advances in Chemical Physics*, edited by I. Prigogine and S. A. Rice (Wiley, New York, 1982).
[20]F. H. Stillinger and A. Rahman, J. Chem. Phys. **60**, 1545 (1974).
[21]J. L. Lebowitz, J. K. Percus, and L. Verlet, Phys. Rev. **153**, 250 (1967).
[22]A. Rahman and F. H. Stillinger, J. Chem. Phys. **55**, 3336 (1971).
[23]H. Harder, Ph.D.-Thesis, Universität Karlsruhe (1972).
[24]K. Krynicki, S. N. Changdar, and J. C. Powles, Mol. Phys. **39**, 773 (1980).
[25](a) K. Krynicki and J. G. Powles, J. Magn. Res. **6**, 539 (1972); (b) J. G. Powles and M. Rhodes, Phys. Lett. A **24**, 523 (1967).
[26]J. G. Powles, E. K. Oase, J. C. Dore, and P. Chieux, Mol. Phys. **43**, 1051 (1981).
[27]J. P. Perchard, W. F. Murphy, and J. H. Bernstein, Mol. Phys. **23**, 499 (1971).
[28]E. Sander and R. F. C. Farrow, Nature (London) **213**, 171 (1967).
[29](a) K. Mangold and E. U. Franck, Zeitschrift für Elektro chemie **66**, 260 (1962); (b) E. U. Franck, M. Bose, and K. Mangold in Prog. Intern. Res. Thermodynamic Transport Papers, 2nd Symp. Thermophysical Properties, Princeton, N.Y., 159 (1962).